References and Notes

1. J. E. Titheridge, *Planet. Space Sci.* **20**, 353 (1972).
2. Operated by the Air Force Cambridge Research Laboratories (AFCRL), Hanscom Air Force Base, Bedford, Massachusetts.
3. M. Mendillo, G. S. Hawkins, J. A. Klobuchar, *Tech. Rep. TR-74-0342, ERP 483* (Air Force Cambridge Research Laboratories, Hanscom Air Force Base, Bedford, Massachusetts, July 1974).
4. M. Mendillo and J. A. Klobuchar, *Tech. Rep. TR-74-0065* (Air Force Cambridge Research Laboratories, Hanscom Air Force Base, Bedford, Massachusetts, 1974).
5. G. T. Pinson, *Tech. Rep. D5-15560-13* (Boeing Company, Huntsville, Alabama, 1973).
6. S. A. Sadunas, E. P. French, H. Seaton, *NASA Contractor Rep. 129009* (Rockwell International Corporation, Downey, California, 1973).
7. H. Rishbeth and O. K. Garriott, *Introduction to Ionospheric Physics* (Academic Press, New York, 1969), chap. 3.
8. E. E. Ferguson, *Atomic Data Nuclear Data Tables* **12**, 159 (1973). Ferguson quotes as rate constants for Eqs. 1 and 2, respectively, 2.0×10^{-9} cm³/sec and 2.4×10^{-9} cm³/sec, ± 30 percent.
9. P. M. Banks and G. Kockarts [*Aeronomy* (Academic Press, New York, 1973), part A, chap. 10] point out that the dissociative recombination rate constants are of the order of 10^{-7} cm³/sec.
10. The loss of the TEC is usually described by

$$\frac{d\,\mathrm{TEC}}{dt} = -\beta_{eff}\,\mathrm{TEC}$$

where the effective loss coefficient (β_{eff}) is typically equal to 2×10^{-5} to 4×10^{-5} sec^{-1}. It is determined from theory, or from observations after sunset when solar production ceases and the TEC slowly decays to low nighttime values.
11. W. Jost, *Diffusion* (Academic Press, New York, 1960), chap. 1.
12. The exact relationship

$$t_{max} = \frac{1}{6}\frac{r^2}{D}$$

is obtained by setting the time derivative of Eq. 6 equal to zero. For H_{2^+} it numerically becomes $t_{max} \approx 3/4\ r^2$, where t_{max} is in minutes and r is in hundreds of kilometers.
13. In the more rigorous treatment (*3*), the TEC is evaluated using

$$d\mathrm{TEC}(t)/dt = Q - [\beta_{eff} + \beta_{H_2}(t) + \beta_{H_2O}(t)]\ \mathrm{TEC}(t)$$

where Q is a modified production function obtained from the average rate of change of TEC prior to the launch.
14. E. E. Ferguson, personal communication.

15. We thank Dr. J. Aarons of the Ionospheric Physics Laboratory (AFCRL) for his encouragement and support. We thank Dr. W. Swider (AFCRL) who provided valuable assistance concerning the aeronomic processes involved in this study, and S. Sadunas (Rockwell International, Downey, California) and C. Varnardo (NASA, Huntsville, Alabama) who kindly furnished the answers to various technical questions concerning Saturn V launches. M.M. was supported under a National Research Council–National Academy of Sciences resident research associateship at AFCRL (1972–1974). G.S.H. is currently at AFCRL as senior resident research associate with the support of the National Research Council–National Academy of Sciences, on leave from the Smithsonian Astrophysical Observatory.

16 September 1974; revised 25 October 1974 ■

Seasonal Change of Antarctic Sea Ice Cover

Abstract. *The winter expansion of the sea ice surrounding Antarctica and the subsequent retreat of the ice in summer may be linked with the wind stress acting on the Southern Ocean in conjunction with the heat exchange in open water regions within the ice fields.*

The Antarctic sea ice undergoes immense seasonal fluctuations in areal extent (Fig. 1). The maximum area, 22×10^6 km², occurs in September and the minimum, 4×10^6 km², in March (*1*). Although other estimates differ slightly (*2, 3*), all indicate seasonal variations of approximately 18×10^6 km², an area larger than that of Antarctica and its ice shelves.

Sea ice acts as an insulator, effectively reducing radiative and nonradiative heat flux between ocean and atmosphere (*4*). In summer, when incoming solar radiation is large, the ice reflects 40 to 70 percent of this radiation to drastically reduce heating of the ocean; if the ocean were ice-free it would reflect only 10 percent (*4*). In winter the ice cuts down substantially on the sensible and latent heat flux from ocean to atmosphere, because of its low heat conductivity and low vapor pressure (*4*).

Sea ice, with a salinity of 3 to 5 per mil (*5*), is an important factor in the ocean's salt balance, ejecting some 3 g of salt per square centimeter of surface as a cold brine into the ocean for each meter of ice formed. This process reduces the stability of the ocean surface layer and convection can ensue. The convection may penetrate the relatively warm-saline upper layers of circumpolar deep water (400 to 600 m deep), which would result in a significant upward heat flux into the surface layers and eventually into the atmosphere (*6, 7*). During ice melting the release of relatively fresh water increases the stability of the surface layer, retarding convection.

Hence, the seasonal variation of the ice has important effects on the thermohaline structure of the ocean and on the characteristics of the atmosphere. The reason for the large seasonal change has not been investigated; presumably new ice is added in winter to the outer fringes of the sea ice field and removed the following summer. We present the hypothesis that much of the ice growth and retreat is due to processes related to the wind stress within the sea ice fields.

The curl of the wind stress (*8*), which induces a general Ekman divergence of surface water and sea ice cover, continuously generates open water regions with freezing point temperatures within the ice fields. In winter the open water fills with new ice and the ice field expands accordingly, extending northward as a function of the total divergence within the existing ice field. The northern extent of the ice may be determined by an inability of the local heat balance (in both atmosphere and ocean) to continually freeze over the open water generated by the Ekman divergence. The resulting partial ice cover may then be destroyed by ocean waves which penetrate into the ice field. After the spring equinox, open water regions within the ice field increase heat absorption by the ocean, and rapid ice melting follows.

The hypothesis can be evaluated by comparing the observed winter growth rate of the ice with the rate calculated from the Ekman divergence. Figure 1 indicates an observed growth rate (mid-March to mid-August) of 3.3×10^6 km² per month.

The rate of divergence of the ice can only be estimated, since understanding of the behavior of ice on a boundary layer is incomplete, although one would anticipate less interference of ice with the ocean-atmosphere coupling in a divergent Ekman field (*9*). In view of these uncertainties we cannot firmly establish the validity of our hypothesis. However, we can test to see if it is reasonable.

The total Ekman transport is directed at a right angle to the surface wind direction and is proportional to the ratio of wind stress to Coriolis parameter (*10*). However, the full magnitude of the drift is accounted for in the upper half of the Ekman layer, and is directed 78° to the left of the wind direction in the Southern Hemisphere. Below this segment of the Ekman layer the contribution to the total drift vector is a further 12° rotation to the left of the wind direction. Therefore, the total divergence is calculated by assuming uniform horizontal flow in the upper half of the Ekman layer. The Ekman is taken to be equivalent to the thickness of the mixed layer (*11*), which in the ice field is about 40 m (*7*). The data in

Fig. 2 indicate an average annual vertical velocity (for the points at and to the south of the maximum upwelling) of 10×10^{-5} cm/sec for the western section, and 17×10^{-5} cm/sec for the eastern section. The April values (introduced since this represents the waxing period) are a bit larger: 12×10^{-5} and 18×10^{-5} cm/sec, respectively. Using a characteristic value of 14×10^{-5} cm/sec, we calculate the monthly ice growth as equal to the area determined by the surface divergence. The ice covers an increasing area and therefore grows at an increasing rate (Fig. 1).

The calculated rates are less than the observed rates, but a number of factors must be considered.

1) The model presented is not strictly valid in March and April, when the ice field is essentially nonexistent. In these months the ice field is most likely initiated as thin sheets close to Antarctica. Once this initial ice field forms, the model presented above becomes an increasingly important factor in the further northward expansion of the ice.

2) The wind stress was calculated according to the bulk aerodynamic equations (*8*) with the average geostrophic wind velocity, which was then squared. This yields a smaller value than would be obtained if the average of the square of the geostrophic wind speed were used. To compensate, Roden (*12*) doubled the drag coefficient to 2.6×10^{-3}. The higher value would have the effect of doubling the divergence and ice growth. The growth rate based on data for April and the drag coefficient of 2.6×10^{-3} coincides well with the observed increase to mid-July. However, the mean geostrophic wind velocity is greater than the real wind velocity (*13*) and at least partially alleviates the need for increasing the drag coefficient. Statistical wind data (*14*) show that the mean geostrophic wind velocities (*13*) are sufficiently greater than the observed wind velocities to warrant use of 1.3×10^{-3} for the drag coefficient.

3) In the western Weddell Sea ice is advected northward, then eastward along 60°S (*1*). This special case is not included in the model. The area of ice carried northward in the Weddell Sea in this way may be 3×10^6 to 5×10^6 km^2, based on the residual tongue of ice along 60°S in the western Atlantic observed in the early summer months (*1*). This area must be subtracted from the total to better evaluate the model. If 4×10^6 km^2 of ice can be accounted for by advection, and if it occurs uniformly from mid-March to mid-August, the observed growth rate would be 2.5×10^6 rather than 3.3×10^6 km^2 per month, which compares well with the calculated growth rates based on April and May data and the lower drag coefficient.

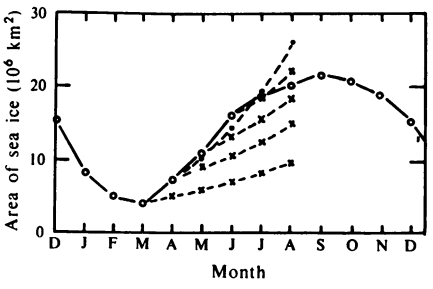

Fig. 1. (○) Annual fluctuation of Antarctic sea ice based on mid-month values (*1*). The other curves show the sea ice area during advance, based on the Ekman divergence model with a drag coefficient of 1.3×10^{-3} (X) or 2.6×10^{-3} (○) (*8*). Each curve begins with the month for which the observed ice cover is used to initiate the calculations.

In view of the limitations discussed above, we can only state that the calculations suggest a probability that the curl of the wind stress and the associated Ekman divergence, in conjunction with the heat balance, may account for the immense expansion of the Antarctic sea ice in winter. The rapid decay of the ice in summer would also be related to these factors, when the generation of open water acts as a heat source for the ocean.

The curl of the wind stress is associated with cyclones, and these are most frequent over the maximum upwelling belt (*15*), which coincides with the maximum limit of the sea ice. Yearly variability in the frequency and path of cyclones would affect the generation of open water and hence the seasonal fluctuations of the ice. A more northern position for the cyclone belt would allow greater northern expansion of the ice and decrease upwelling to the south, which would limit the extent of summer melting and therefore reduce the seasonal fluctuations of the ice.

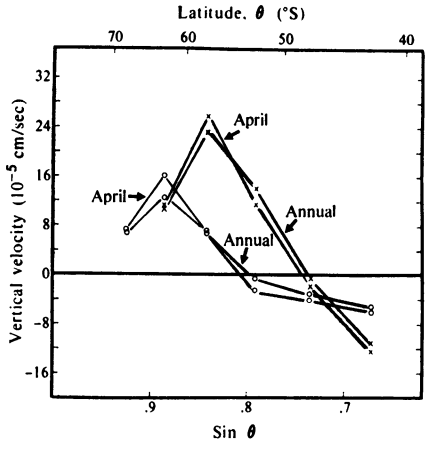

Fig. 2. Zonally averaged annual mean values and April values of the vertical velocity induced by the Ekman divergence, calculated from average wind speed data (*13*). The linear scale used is $\sin\theta$ since the area between parallels is proportional to $\Delta\sin\theta$. Zonal analyses are done for two regions because of the asymmetry of upwelling: 20°W eastward to 155°E (X) and 160°E eastward to 25°W (○).

ARNOLD L. GORDON
HOYT W. TAYLOR
Lamont-Doherty Geological Observatory and *Department of Geological Sciences of Columbia University, Palisades, New York 10964*

References and Notes

1. N. A. Mackintosh, *Discovery Rep.* **36**, 1 (1972).
2. A. F. Treshnikov, *Proceedings of the Symposium on Pacific-Antarctic Sciences*, Y. Nagata, Ed. (Tokyo National Science Museum, Tokyo, 1967), p. 7.
3. N. A. Streten, *Arch. Meteorol. Geophys. Bioklimatol. Ser. A Meteorol. Geophys.* **22**, 119 (1973).
4. J. O. Fletcher, *Rand Corp. Memo RM-5793-NSF* (1969), pp. 1–108.
5. G. Neumann and W. J. Pierson, Jr., *Principles of Physical Oceanography* (Prentice-Hall, Englewood Cliffs, N.J., 1966).
6. A. F. Treshnikov, A. O. Shaikher, B. V. Gindysh, *Probl. Arktiki Antarktiki No. 27* (1967), pp. 35–47; a translation appears in (*4*, pp. 85–99).
7. A. L. Gordon, H. W. Taylor, D. T. Georgi, paper presented at the SCOR-SCAR (Scientific Committee on Oceanographic Research–Scientific Committee on Antarctic Research) Polar Oceans Conference, McGill University, Montreal, Canada, 5 to 11 May 1974.
8. The curl of the wind stress is $\partial\tau x/\partial y - \partial\tau y/\partial x$, where τx and τy are the components of wind stress acting on the ocean surface in the eastern and northern directions, respectively. The winds stress is given by the aerodynamic equations
$$\tau x = \rho_{air} C_D W_x (W_x^2 + W_y^2)^{1/2}$$
$$\tau y = \rho_{air} C_D W_y (W_x^2 + W_y^2)^{1/2}$$
where ρ_{air} is the density of the air, C_D is the drag coefficient, and W_x and W_y are the wind velocity components in the eastern and northern directions, respectively.
9. J. A. Galt, *J. Phys. Oceanogr.* **3**, 379 (1973).
10. V. W. Ekman, *Ark. Mat. Astron. Fys.* **2** (No. 11) (1905).
11. R. T. Pollard, P. B. Rhines, R. O. R. Y. Thompson, *Geophys. Fluid Dyn.* **3**, 381 (1973).
12. G. Roden, *J. Phys. Oceanogr.* **4**, 168 (1974).
13. R. L. Jenne, H. Crutcher, H. van Loon, J. J. Taljaard, *Climate of the Upper Air: Southern Hemisphere* (NCAR-TN/STR-58, National Center for Atmospheric Research, Boulder, Colo., 1971), vol. 3.
14. *U.S. Navy Marine Climatic Atlas of the World* (Navweps 50-IC-50, Government Printing Office, Washington, D.C., 1965), vol. 7.
15. J. J. Taljaard, *Meteorol. Monogr.* **13**, 139 (1972).

16. We acknowledge NSF/IDOE grant GX-41955. Lamont-Doherty Geological Observatory Contribution No. 2182.

19 August 1974; revised 15 October 1974